

Thermodynamic properties of the periodic Anderson model : X-boson treatment

R. Franco* and M. S. Figueira†

*Instituto de Física, Universidade Federal Fluminense (UFF),
Av. Litorânea s/n, 24210-340 Niterói,
Rio de Janeiro, Brazil, Caixa Postal 100.093*

M. E. Foglio‡

*Instituto de Física “Gleb Wataghin”,
Universidade Estadual de Campinas, 13083-970 Campinas,
São Paulo, Brazil, Caixa Postal 6165*

(Dated: November 3, 2018)

Abstract

We study the specific heat dependence of the periodic Anderson model (PAM) in the limit of $U = \infty$ employing the X-boson treatment in two different regimes of the PAM: the heavy fermion Kondo (HF-K) and the local magnetic moment regime (HF-LMM). We obtain a multiple peak structure for the specific heat in agreement with the experimental results as well as the increase of the electronic effective mass at low temperatures associated with the HF-K regime. The entropy per site at low T tends to zero in the HF-K regime, corresponding to a singlet ground state, and it tends to $k_B \ln 2$ in the HF-LMM, corresponding to a doublet ground state at each site. The linear coefficient $\gamma(T) = C_v(T)/T$ of the specific heat qualitatively agrees with the experimental results obtained for different materials in the two regimes considered here.

PACS numbers: 71.10.-w, 71.27.+a, 71.28.+d, 75.20.Hr, 75.30.Mb, 75.40.Cx

I. INTRODUCTION

Heavy fermions metals (HF) are intermetallic compounds of certain lanthanides and actinides. They contain a lattice of f ions, embedded in a Fermi sea of conduction electrons c . These materials exhibit very large specific heats and spin susceptibilities at low temperatures, and these characteristics are associated with high effective masses of quasi-particles, caused by the local strong Coulomb interaction between the f electrons. The periodic Anderson model (PAM) is considered a fairly good description of these systems, and the relevant parameters of this model are: the hybridization V between the localized f -electrons and the itinerant c electrons (associated with the s , p and d orbitals), the value of the energy E_f of the localized f level, the value U that determines the Coulomb repulsion energy between the f electrons, the dispersion relation of the c -electrons and the chemical potential μ . The physics of these materials is dominated by the competition between the Kondo effect, that tends to quench the magnetic moments of the f levels,¹ and the RKKY (Rudermann-Kittel-Kasuya-Yosida) interaction, that tends to introduce antiferromagnetic order in the lattice.^{2,3} Some of these compounds develop superconducting states at low temperatures, and their nature is not yet completely understood.^{4,5}

The thermodynamic properties of the PAM have been recently studied employing different methods: equation of motion (EOM)^{6,7} and two variants of the mean field theory⁸ that respectively describe the weak coupling limit (Hartree-Fock) and the strong coupling one (slave boson mean field theory (SBMFT)^{9,10,11}). An interesting result in all these works^{6,7,8} is the presence of a multiple peak structure in the temperature dependence of the specific heat. In the works that use the EOM, the first peak was associated with spin fluctuations and the second one with charge fluctuations^{6,7}. Bernhard et.al.⁶, defined a lattice Kondo temperature T_K (we call it T_{KL} in this work) as equal to the T corresponding to the minimum of the temperature derivative of the average $\langle c_{i\sigma}^\dagger f_{i\sigma} \rangle$, that measures the “transference” of electrons from the localized levels to the conduction band and vice-versa. On the other hand, Peres et.al.⁸, define a correlation temperature T^* (we call it T_0 in this work) equal to the T corresponding to the maximum of the temperature derivative of the parameter $\langle c_{i\sigma}^\dagger f_{i\sigma} \rangle$. As they employ the SBMFT the dynamical fluctuations do not appear explicitly in their Green’s Functions (GF), and they concluded that the multiple peak structure of the specific heat is only associated with band shape effects. We believe that there is no antagonism

between these two explanations: the dynamical fluctuations modify the bands (even in the SBMFT through their mean field contributions to the GF), and it is their spectral densities near the Fermi surface that determine the specific heat.

The dynamical mean field theory¹² (DMFT), with the help of the numerical renormalization group (NRG), has been recently employed to study the PAM¹³ and the Kondo lattice.¹⁴ These works establish the simultaneous existence of two scales of energy: one high temperature scale associated with conventional Kondo scattering and a lower temperature scale, usually called coherence temperature, that is associated with the formation of quasi-particles with strongly enhanced effective masses.¹³ The same result has been also obtained by applying the SBMFT in the large- N approach to the Kondo lattice.¹⁵ The notation of these temperature scales is not uniform in the literature, and we shall then use T_0 for the lattice coherence temperature,^{13,14} and introduce T_{KL} for the high temperature scale, leaving T_K for the impurity Kondo temperature.

In the present work we study the thermodynamic properties of the PAM in the limit of $U \rightarrow \infty$ employing the X-boson method^{16,17,18} in two regimes of the PAM: the heavy fermion Kondo regime (HF-K) and the local magnetic moment regime (HF-LMM).^{4,5} The spurious second order phase transitions of the slave-boson approach,^{16,19} at intermediate temperatures and when $E_f \ll \mu$, are not present in the X-boson method. This method also includes explicitly some temporal quantum fluctuations in the GF,¹⁶ and we analyze some possible consequences of this difference. We show that the parameters T_0 and T_{KL} are determined by the position of the maximum of C_V vs. T , and we discuss the physical origin of these maxima. We show that at low T the entropy per site tends to zero in the HF-K regime, corresponding to a singlet ground state, while it tends to $k_B \ln 2$ in the HF-LMM, corresponding to a doublet ground state at each site and opening the way for the possible formation of an antiferromagnetic order (AF) at low temperatures ($T < T_0$). We show that when the system is in the HF-K regime and the system goes at low temperatures through the Kondo resonance, there is a huge increase of the effective mass of the f electrons, associated with the linear coefficient γ_o of the specific heat. Our calculations of $\gamma(T) = C_v/T$ qualitatively agree with the experimental results at low temperatures for some materials classified in the two regimes considered.

II. MODEL AND METHOD

To study the PAM Hamiltonian in the $U = \infty$ limit, the f -levels with double occupation are projected out from the space of the local states by employing the Hubbard X operators,^{20,21,22} and we obtain

$$H = \sum_{\mathbf{k},\sigma} \varepsilon_{\mathbf{k},\sigma} c_{\mathbf{k},\sigma}^\dagger c_{\mathbf{k},\sigma} + \sum_{\sigma,f} E_{f,\sigma} X_{f,\sigma\sigma} + \sum_{\mathbf{k},\sigma} \left(V_{f,\mathbf{k},\sigma} X_{f,0\sigma}^\dagger c_{\mathbf{k},\sigma} + V_{f,\mathbf{k},\sigma}^* c_{\mathbf{k},\sigma}^\dagger X_{f,0\sigma} \right). \quad (1)$$

The first term of the equation represents the Hamiltonian of the conduction electrons (c -electrons), associated with the itinerant electrons (s , p and d orbitals). The second term describes the localized f levels and the last one corresponds to the interaction between the c -electrons and the f -electrons via hybridization between the f and c states. This Hamiltonian can be treated by the X-boson approach^{16,17,18} for the lattice case, and the cumulant Green's function (GF) are then given by

$$G_{\mathbf{k}\sigma}^{ff}(z) = \frac{-D_\sigma (z - \varepsilon_{\mathbf{k}\sigma})}{\left(z - \tilde{E}_{f,\sigma} \right) (z - \varepsilon_{\mathbf{k}\sigma}) - |V_\sigma(\mathbf{k})|^2 D_\sigma}, \quad (2)$$

$$G_{\mathbf{k}\sigma}^{cc}(z) = \frac{-\left(z - \tilde{E}_{f,\sigma} \right)}{\left(z - \tilde{E}_{f,\sigma} \right) (z - \varepsilon_{\mathbf{k}\sigma}) - |V_\sigma(\mathbf{k})|^2 D_\sigma}, \quad (3)$$

and

$$G_{\mathbf{k}\sigma}^{fc}(z) = \frac{-D_\sigma V_\sigma(\mathbf{k})}{\left(z - \tilde{E}_{f,\sigma} \right) (z - \varepsilon_{\mathbf{k}\sigma}) - |V_\sigma(\mathbf{k})|^2 D_\sigma}, \quad (4)$$

where $z = \omega + i\eta$, with $\eta \rightarrow 0^+$. The correlations appear in the chain X-boson approach through the quantity $D_\sigma = R + n_{f,\sigma}$, where $R = \langle X_{0,0} \rangle$. This simple factor introduces essential differences with the MFSBT^{16,17} and these GF can not be transformed into those of two hybridized bands of uncorrelated electrons with renormalized parameters, as it is done in the MFSBT. A renormalized $\tilde{E}_f = E_f + \Lambda$ also appears here in the X-boson method, with Λ given by

$$\Lambda = \frac{1}{N_s} \sum_{\mathbf{k},\sigma} |V_\sigma(\mathbf{k})|^2 \times \frac{n_F(\omega_{\mathbf{k},\sigma}(+)) - n_F(\omega_{\mathbf{k},\sigma}(-))}{\sqrt{\left(\varepsilon_{\mathbf{k},\sigma} - \tilde{E}_{f,\sigma} \right)^2 + 4 |V_\sigma(\mathbf{k})|^2 D_\sigma}}, \quad (5)$$

where $n_F(x)$ is the Fermi-Dirac distribution and N_s is the number of sites. To simplify the calculations we shall consider a rectangular conduction band of width $W = 2D$, centered at the origin, and a real hybridization constant $V_\sigma(\mathbf{k}) = V$. We then obtain

$$\Lambda = \frac{V^2}{D} \int_{-D}^D d\varepsilon_{\mathbf{k}} \frac{n_F(\omega_{\mathbf{k}}(+)) - n_F(\omega_{\mathbf{k}}(-))}{\sqrt{(\varepsilon_{\mathbf{k}} - \tilde{E}_f)^2 + 4V^2D_\sigma}}, \quad (6)$$

where the values $\omega_{\mathbf{k},\sigma}(\pm)$ are the poles of the GF, given by

$$\begin{aligned} \omega_{\mathbf{k},\sigma}(\pm) &= \frac{1}{2} (\varepsilon_{\mathbf{k},\sigma} + \tilde{E}_f) \\ &\pm \frac{1}{2} \sqrt{(\varepsilon_{\mathbf{k},\sigma} - \tilde{E}_f)^2 + 4V^2D_\sigma}. \end{aligned} \quad (7)$$

In the X-boson approach $D_\sigma = R + n_{f\sigma}$ must be calculated self-consistently through the minimization of the corresponding thermodynamic potential with respect to the parameter R . When the total number of electrons N_{tot} , the temperature T and the volume V_s are kept constant one should minimize the Helmholtz free energy F , but the same minimum is obtained by employing the thermodynamic potential $\Omega = -k_B T \ln(\mathcal{Q})$, (where \mathcal{Q} is the Grand Partition Function) while keeping T , V_s , and the chemical potential μ constant (this result is easily obtained by employing standard thermodynamic techniques). In the X-boson method the grand thermodynamic potential is^{16,17}

$$\begin{aligned} \Omega &= \bar{\Omega}_0 + \frac{-1}{\beta} \sum_{\mathbf{k},\sigma,\pm} \ln [1 + \exp(-\beta \omega_{\mathbf{k},\sigma}(\pm))] \\ &+ N_s \Lambda(R - 1), \end{aligned} \quad (8)$$

where

$$\bar{\Omega}_0 = -\frac{N_s}{\beta} \ln \left[\frac{1 + 2 \exp(-\beta \tilde{E}_f)}{(1 + \exp(-\beta \tilde{E}_f))^2} \right], \quad (9)$$

$\beta = 1/k_B T$, and k_B is the Boltzmann constant. By standard thermodynamic techniques we find

$$S = - \left(\frac{\partial F}{\partial T} \right)_{N_{tot}, V_s} = - \left(\frac{\partial \Omega}{\partial T} \right)_{\mu, V_s}, \quad (10)$$

and

$$\begin{aligned} C_v &= T \left(\frac{\partial S}{\partial T} \right)_{N_{tot}, V_s} = -T \left(\frac{\partial^2 \Omega}{\partial T^2} \right)_{\mu, V_s} \\ &+ T \left(\frac{\partial \mu}{\partial T} \right)_{N_{tot}, V_s} \left(\frac{\partial N_{tot}}{\partial T} \right)_{\mu, V_s}. \end{aligned} \quad (11)$$

For the rectangular conduction band we find from Eqs. (8,9) that, in the absence of magnetic field,

$$\begin{aligned}
& -T \left(\frac{\partial^2 \Omega}{\partial T^2} \right)_{\mu, V_s} = -T \left(\frac{\partial^2 \bar{\Omega}_0}{\partial T^2} \right)_{\mu, V_s} \\
& + \frac{k_B \beta^2}{D} \sum_{\ell=\pm}^2 \int_{-D}^D dx \omega_{\ell}^2(x) n_F(\omega_{\ell}(x)) [1 - n_F(\omega_{\ell}(x))] \\
& - T N_s \left(\frac{\partial^2 (\Lambda(R-1))}{\partial T^2} \right)_{\mu, V_s}, \tag{12}
\end{aligned}$$

where

$$\omega_{\pm}(x) = \frac{1}{2} \left(x + \tilde{E}_f \right) \pm \frac{1}{2} \sqrt{\left(x - \tilde{E}_f \right)^2 + 4 |V|^2 D_{\sigma}} \tag{13}$$

and

$$\begin{aligned}
& -T \left(\frac{\partial^2 \bar{\Omega}_0}{\partial T^2} \right)_{\mu, V_s} = -2N_s k_B \beta^2 \tilde{E}_f^2 \exp(\beta \tilde{E}_f) \\
& \times \frac{[3 + 2 \exp(\beta \tilde{E}_f)]}{\left[\exp(\beta \tilde{E}_f) + 2 \right]^2 \left[\exp(\beta \tilde{E}_f) + 1 \right]^2}. \tag{14}
\end{aligned}$$

We have calculated $T (\partial\mu/\partial T)_{N_{tot}, V_s}$ $(\partial N_{tot}/\partial T)_{\mu, V_s}$ numerically.

III. RESULTS AND DISCUSSION

A schematic classification for typical Ce-based compounds was given earlier by Varma²³ and reintroduced by Steglich et. al.^{4,5} in terms of the dimensionless coupling constant for the exchange between the local f spin and the conduction-electron spins, $g = N_F |J|$, where N_F is the conduction-band density of states at the Fermi energy and J is connected to the parameters of the PAM via a Schrieffer-Wolff transformation,²⁴ $J = |2V^2 / (E_f - \mu)|$ (for $U \rightarrow \infty$). The behavior of these compounds can then be qualitatively organized through the parameter

$$g = 2V^2 \rho_c(\mu) / |E_f - \mu|, \tag{15}$$

where $\rho_c(\mu) = 1/2D$ is independent of μ in our case, E_f is the bare localized f level and we employ the chemical potential μ obtained in the self-consistent X-boson calculation for the total number of particles per site $n_{tot} = 2(n_{f,\sigma} + n_{c,\sigma})$ at the very low temperature $T = 0.0001D$.

When $g > 1$, the compound under consideration is in the intermediate valence (IV) region, while for $g < 1$ it is in the heavy fermion Kondo regime (HF-K). There exists a critical value g_c at which the Kondo and the RKKY interactions have the same strength, and non Fermi-liquid (NFL) effects have been postulated for systems with $g = g_c$. For $g_c < g < 1$ the magnetic local moments are quenched at very low temperatures and the system presents a Fermi liquid behavior, while for $g < g_c$ we have the local magnetic moment regime (HF-LMM). We point out that the parameter g classifies the regimes of the PAM only in a qualitative way. Finally, as in its present form the X-boson approach includes hybridization effects only to second order in V and the self-energy does not depend on the wave vector,¹⁶ the RKKY effects are not present and we cannot discuss non Fermi-liquid behavior within the present approximation, nor find the value of g_c .

A. Results for the HF- regime

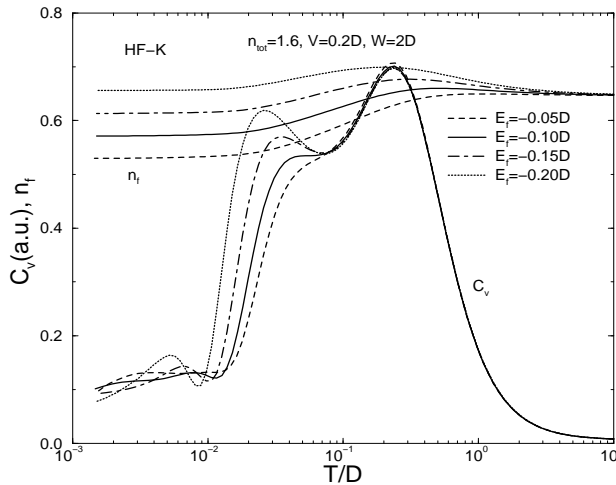


FIG. 1: Specific heat C_V and occupation of the localized f levels n_f vs. temperature T , for the HF-K regime. Notice that the intensity of the two maxima of C_V at lower T first decreases and then disappears when the number $n_c = 1.6 - n_f$ of conduction electrons increases, while their positions T_0 and T_{KL} shift to the right.

In Fig. 1 we show the specific heat C_v and the occupation n_f of the localized level as a function of the temperature T for several sets of parameters that describe a HF-Kondo situation (HF-K): hybridization $V = 0.2D$, total number of particles per lattice site $n_{tot} = 1.6$ and bandwidth $W = 2D$; the bare localized energy levels E_f employed and the corresponding

Steglich's parameters^{4,5,25} g (for $T = 0.0001D$) are $E_f = -0.05D$, $g = 0.426$; $E_f = -0.10D$, $g = 0.392$; $E_f = -0.15D$, $g = 0.365$ and $E_f = -0.20D$, $g = 0.342$. In Fig. 2 we plot both the f and c spectral densities for $E_f = -0.15D$, showing the high density of states f at the chemical potential for that set of parameters.

FIG. 2: The f and c electronic density of states $\rho_{f,\sigma}(\omega)$ and $\rho_{c,\sigma}(\omega)$ vs. ω at low temperatures, for the HF-K regime. The position of the renormalized energy level $\tilde{E} = E_f + \Lambda$ and of the chemical potential μ are shown. Similar results were obtained for other set of parameters in the same regime.

In Fig. 3 we plot the specific heat, the entropy and the total occupation of the f level as a function of T for the same set of parameters of Fig. 2. We can see that the entropy S per site tends to zero at low temperatures, and we conclude that the system goes to the Kondo singlet ground-state, while the huge value of density of states f at the chemical potential μ (see figure 2) signals the simultaneous appearance of the Kondo resonance. The inset shows, in agreement with reference 15, that an entropy approximately equal to $n_c k_B \ln(2)$ is lost below T_{KL} .

At high temperatures the system behaves like a collection of independent f and c electrons, because both $V/k_B T$ and $D/k_B T$ tend to zero like $1/T$. For a system with a chemical potential that remains finite when $T \rightarrow \infty$ the entropy per site would tend to $k_B \ln(12)$, corresponding to the dimensionality of the purely local Hilbert space, but this result is not true any more when we keep fixed the total number of electrons per site n_{tot} , as discussed in more detail in Appendix A. The value of the entropy when $n_{tot} = 1.6$ (the value employed in figures 1-6) is equal to $0.998765 k_B \ln 12$ and is indistinguishable from $k_B \ln(12)$ in the

figures.

FIG. 3: Entropy S , Specific heat C_v and total occupation of the localized levels n_f vs. T , for the same set of parameters of Fig. 2. The behavior of the curves is similar for other parameters corresponding to the same HF-K regime.

In the Fig. 4 we plot the specific heat C_v , the chemical potential μ , the temperature derivative of the parameter $\langle c_{i\sigma}^\dagger f_{i\sigma} \rangle \equiv n_{fc,\sigma}$, the occupation number n_f of the f levels, and the value at μ of the f density of states $\rho_{f,\sigma}(\mu)$, as a function of T for a system in the HF-K regime. The average $\langle c_{i\sigma}^\dagger f_{i\sigma} \rangle \equiv n_{fc,\sigma}$ is associated with the GF $G_{\mathbf{k}\sigma}^{fc}(z_n)$, and it is a measure of the mixing of the c and f states in the system. We associate the temperatures T_0 and T_{KL} respectively to the maximum and the minimum of the $(dn_{fc,\sigma}/dT)$ (they are named T^* in Peres *et.al.*⁸ and T_K in Bernhard *et.al.*⁶ respectively). They are both shown in the figure, where it is clear that T_0 coincides with the first peak of C_V and T_{KL} with the second one. Only one extreme was observed in previous works.^{6,8}

The chemical potential μ changes with temperature because we keep the total number of particles constant, and in our calculations it shifts into the hybridization gap at intermediate temperatures. The density of states at the chemical potential $\rho_{f,\sigma}(\mu)$ has a very large value at low T , but at $T \sim T_0$ this quantity shows a drastic change with increasing T , taking a value close to zero when μ enters the gap, as shown in Fig. 4. The moderate increase in the average electronic energy that occurs in this process is the origin of the first peak of C_v .

It seems reasonable to use T_0 as a measure of the Kondo lattice temperature, because crossing T_0 (with decreasing T) we find that $\rho_{f,\sigma}(\mu)$ changes from very small to very large

values, and at the same time the entropy takes small values, tending to zero when $T \rightarrow 0$ (cf. Fig. 3). These two properties characterize respectively the appearance of the Kondo peak and the formation of a singlet by the quenching of the magnetic moment of the f electrons by the cloud of c electrons, and our choice of T_0 as the crossover parameter seems reasonable.

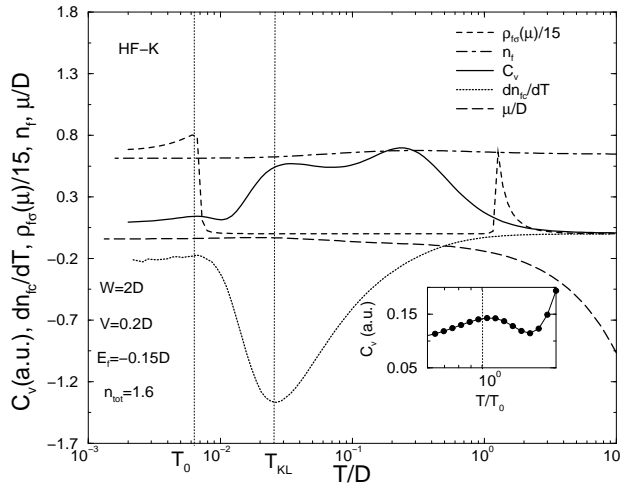


FIG. 4: Specific heat C_v , chemical potential μ , density of states $\rho_{f,\sigma}(\mu)$ of the f -electrons at μ , $(dn_{f,c,\sigma}/dT)$, and n_f vs. T , for the same set of parameters given in Fig. 1 but with $E_f = -0.15D$. We indicate the temperatures T_0 ⁸ and T_{KL} .⁶ The inset shows the little peak in C_v at $T = T_0$. The behavior for other sets of parameters corresponding to the same regime is similar.

The temperatures T_0 and T_{KL} coincide in our treatment with the first two peaks of C_V , and correspond to the two energy scales that appear in the DMFT treatment of both the PAM¹³ and of the Kondo lattice.¹⁴ The lattice coherence scale is associated in the first reference¹³ to the inverse effective mass at the Fermi surface, which in our treatment is proportional to the corresponding density of states: as shown in Fig. 4 this quantity develops a very large increase when T decreases below T_0 . This same scale is also associated in the second reference¹⁴ to the onset of Fermi-liquid coherence, and can be determined from various dynamical quantities including the f -electron Kondo resonance.²⁶ It should be remarked that the drastic change that $\rho_{f\sigma}(\mu)$ suffers when T crosses T_0 (cf. Fig. 4), is consistent with the result reported in Section 3.5 of reference,¹⁴ that the position of the peak of the resonance, “relative to the chemical potential shifts to below the Fermi level on a scale $\lesssim T_0$ with increasing temperature.”

The second peak at $T = T_{KL}$ corresponds to a second and larger maximum of

$\left|d\langle c_{i\sigma}^\dagger f_{i\sigma}\rangle/dT\right|$, corresponding to the maximum rate of change with T of the mixing between f and c electrons. Even if the GF do not have explicit dynamic fluctuations, the changes in $\left|\langle c_{i\sigma}^\dagger f_{i\sigma}\rangle\right|$ measure a mean-field average of the charge fluctuations, and the peak is due to the energy necessary to change the average occupation of the different types of electrons. The crossover parameter T_{KL} has to be used when $\left|d\langle c_{i\sigma}^\dagger f_{i\sigma}\rangle/dT\right|$ shows a single extreme, as it happens in the half filled symmetric PAM,⁶ because μ is then fixed in the middle of the gap and the changes in population that originated T_0 do not occur.

The temperature T_{KL} corresponds to the second energy scale in both DMFT works,^{13,14} and its corresponding energy is related to the transitions between the states of the pseudo gap that usually appears in that treatment. Our method only gives a real self energy, and we always obtain a real gap rather than a pseudo gap, but the meaning of T_{KL} remains the same. The energy associated to T_{KL} has essentially the same origin as the one corresponding to the Kondo impurity T_K , describing the conventional incoherent Kondo scattering at higher temperatures.¹³ In agreement with the results of several authors,^{13,14,15} T_{KL} decreases when the number n_c of conduction electrons decreases.

Two scales are also found in the large- N SBMFT of the Kondo lattice,¹⁵ characterized by the two maxima of C_V vs. T (though the second maximum is replaced in their Fig. 3b by a discontinuity at the phase transition that appears in the SBMFT at T_{KL}). Although both the model and the treatment are different, the C_V maxima at T_0 in our Fig. 1 have the same trend they show in reference 15, namely that they decrease and finally disappear when the number n_c of conduction electrons increases.

Finally the third peak of C_V is located in a region corresponding to large T , and it measures the energy necessary to take the electrons from the low T distribution into the high temperature limit distribution, that depends on n_{tot} (it would be the uniform distribution for $n_{tot} = 5/3$, cf. Appendix A). As could be expected, the position of the high temperature peak is independent of the value of E_f , as it is shown in figure 1.

In Fig. 5 we plot the coefficient $\gamma(T) = C_V(T)/T$ vs. T for several values of E_f corresponding to the HF-K regime. At low T the coefficient $\gamma(T)$ is proportional to the density of states at the chemical potential μ , and in simple cases this is proportional to the effective mass m^* of the associated quasi-particles. We see in that figure that the value of $\gamma(T)|_{T=0.0} = \gamma_o$ at very low temperatures *has a large increase* when E_f changes from $E_f = -0.05D$ to $E_f = -0.20D$, while the Steglich's parameter respectively decreases from

FIG. 5: Sommerfeld's coefficient $\gamma(T) = C_v(T)/T$ vs. T at very low temperatures for the HF-K regime. We have $\gamma(T)|_{T=0.0} = \gamma_o \propto m^*$, where m^* is the effective mass of the quasi-particles. The two vertical lines delimit the interval of values of T_0 corresponding to the four different curves. In the inset one sees an anomaly in $\gamma(T)$ at $T = T_0$ and verifies that $T^\gamma \ll T_0$ for all the values of E_f .

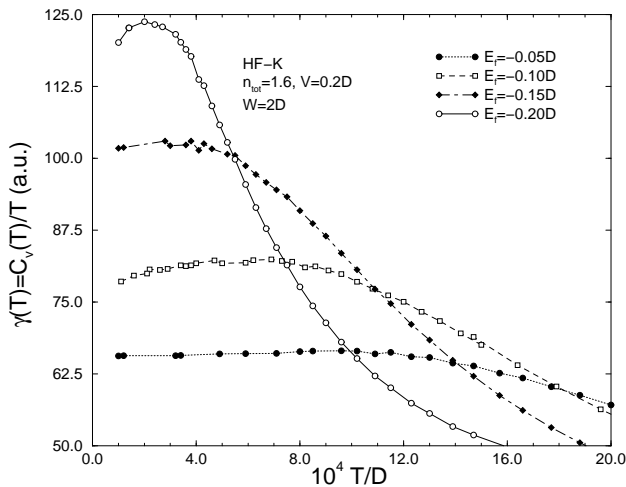


FIG. 6: Sommerfeld's coefficient $\gamma(T) = C_v(T)/T$ vs. T for the HF-K regime, at very low temperatures ($T \sim T^\gamma$).

$g = 0.426$ to $g = 0.342$. This shows that the quasi-particles become heavier as the system evolves in the direction of the Kondo regime. The maximum of $\gamma(T)$ is reached at a value T^γ that satisfies $T^\gamma \ll T_0$. The inset of Fig. 5 shows $\gamma(T)$ vs. T/T_0 for $T/T_0 \sim 1$, and indicates an evident anomaly in $\gamma(T)$ at $T = T_0$ for all the values of E_f in the HF-K param-

eter region. The general form of our results agrees with the experimental measurements for HF systems,^{4,27,28,29,30,31,32} as well as with those of a recent theoretical work.⁷

In Fig. 6 we present the same results of Fig. 5 for very low temperatures showing the maximum of $\gamma(T)$ in detail. The results are qualitatively similar to the experimental measurements for different materials,⁴ like $CeAl_3$ ^{4,28,29,30,32} and $CePtSi$.^{4,31} It is important to emphasize that the best qualitative agreement with the experimental results is given by the set of parameters that corresponds to the highest values of $\rho_{f,\sigma}(\mu)$ at very low temperatures, pointing out the strong HF character of these compounds.

B. Results for the HF-LMM regime

Now we consider several sets of parameters associated with the heavy Fermion local magnetic regime (HF-LMM), defined as before through the Steglich's criterion $g < g_c < 1$,^{4,5} but characterized in our treatment by its properties.²⁵ Our calculations in this regime show that the density of f states at the chemical potential $\rho_{f,\sigma}(\mu)$ for $T \rightarrow 0$ has low values, that the specific heat has a two peak structure, and that the occupation number n_f of localized states is close to 1. In Fig. 7 we plot the same properties given in Fig. 1 for the following set of parameters, that correspond to the HF-LMM regime: hybridization $V = 0.2D$, total number of particles per site $n_{tot} = 1.9$, bandwidth $W = 2D$, and localized energy level given by $E_f = -0.20D$, $E_f = -0.25D$, and $E_f = -0.30D$, corresponding to Steglich's parameters $g = 0.216$, $g = 0.191$, and $g = 0.164$ respectively.

In Fig. 8 we plot both the f and c spectral densities for $E_f = -0.20D$ and $T = 0.001D$, showing the rather small value of the spectral density $\rho_{f,\sigma}(\mu)$ at the chemical potential μ . Notice that in this case (HF-LMM regime) the renormalized energy $\tilde{E}_f = E_f + \Lambda$ is well below the chemical potential μ .

The Fig. 9 is similar to Fig. 3, but for the system in the HF-LMM regime. At very low temperatures the entropy S per site tends to $k_B \ln(2)$, pointing to the transformation of the singlet of the HF-K regime into a ground state consisting of a doublet at each site, that could be attributed to a spin 1/2 at each site. Like in the HF-K regime, the entropy S goes to a high temperature limit that depends only on n_{tot} , as discussed in Appendix A.

In Fig. 10 we present the same results of Fig. 4 for the HF-LMM regime. In this regime the $\rho_{f,\sigma}(\mu)$ goes to zero only in the limit of very high temperatures, because μ is always in

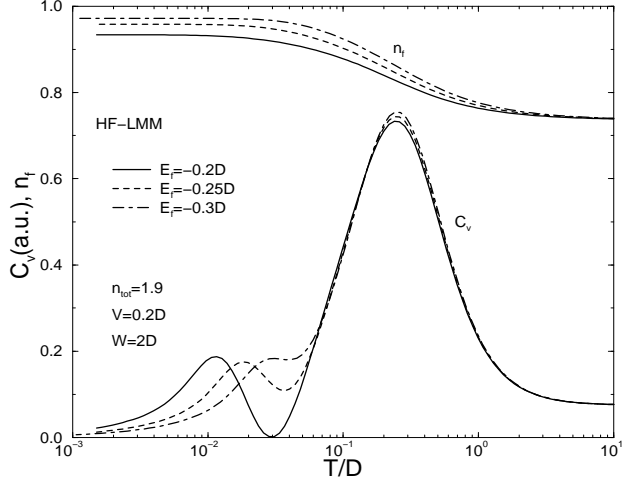


FIG. 7: Specific heat C_v and occupation on the localized f levels n_f vs. temperature T , for the HF-LMM regime.

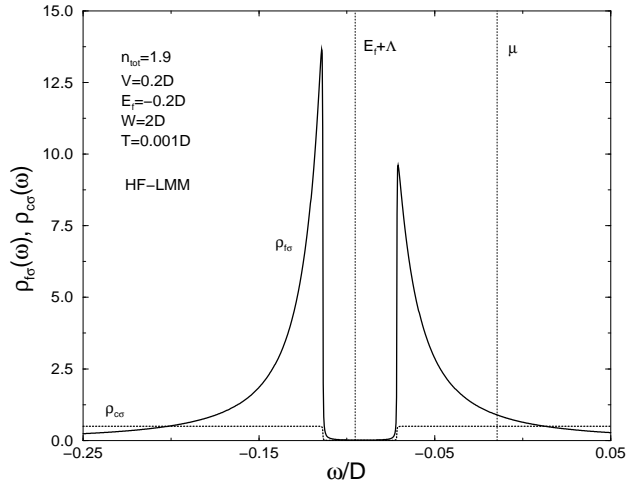


FIG. 8: Density of states $\rho_{f,\sigma}(\omega)$ and $\rho_{c,\sigma}(\omega)$ of f and c electrons as a function of ω at low temperature, for parameters corresponding to the HF-LMM regime. The position of the renormalized energy level $\tilde{E} = E_f + \Lambda$ and of the chemical potential μ are shown. Other sets of parameters in the same regime show a similar behavior.

the tail of the density of states (see figure 8) and does not cross through the gap, as it does in Fig. 4. As a consequence, the peak corresponding to the one at the lowest T in figures 1, 3 and 4 is absent in this regime, and the first specific heat peak that appears is physically equivalent to the one at T_{KL} in the HF-K regime, i.e.: it corresponds to a redistribution of states into higher energies. This C_V peak is less pronounced than in the HF-K region, because many of the low energy states are already occupied at small T because of the larger

value of N_t . The second peak of C_V is now associated with the high temperature limit, and the same arguments employed in the HF-K region apply here; in particular its position is independent of the value of E_f (cf. Fig. 7).

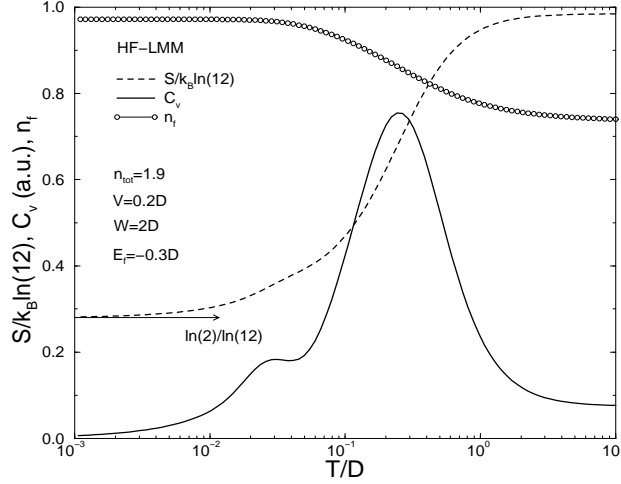


FIG. 9: Entropy S , specific heat C_V and charge at the localized levels n_f vs. T for a set of parameters corresponding to the HF-LMM regime. Other sets of parameters in the same regime show a similar behavior.

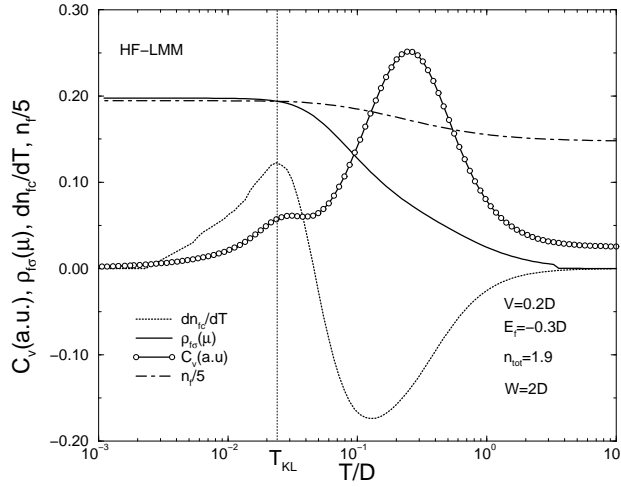


FIG. 10: Specific heat C_V , density of local states $\rho_{f,\sigma}(\mu)$ on the chemical potential μ , dn_{fc}/dT and n_f vs. T , for a set of parameters corresponding to the HF-LMM regime. Only the maximum of dn_{fc}/dT coincides with a maximum of C_V at T_{KL} . Other sets of parameters in the same regime show a similar behavior.

In Fig. 11 we present the same results of Fig. 7 (HF-LMM regime) but with the temperature scaled by T_{KL} . All the first peaks collapse at $T = T_{KL}$ by construction, and the inset

shows a universal cubic dependence of C_v vs. T at low temperatures. The same dependence was obtained by Tesanovic and Valls³³ by starting from the slave boson mean field treatment and considering the interaction between heavy fermions, mediated by fluctuations of the slave bosons. As discussed after equation (A11) in reference 16, the X-boson method retains some time dynamics that is absent in the slave boson method, and this might lead to the same effect obtained by Tesanovic and Valls.

Kim and Stewart³⁴ conclude from their experimental results that, in some heavy Fermion compounds like CeCu₆, a significant contribution to the C_V comes from magnetic correlations. We are not explicitly including magnetic interactions into the model Hamiltonian, and as discussed before, our treatment neither includes the RKKY interaction. Therefore, we can not attribute this T^3 dependence of C_V to intersite magnetic interactions, but it would correspond to Sommerfeld's second term in the C_V temperature expansion.

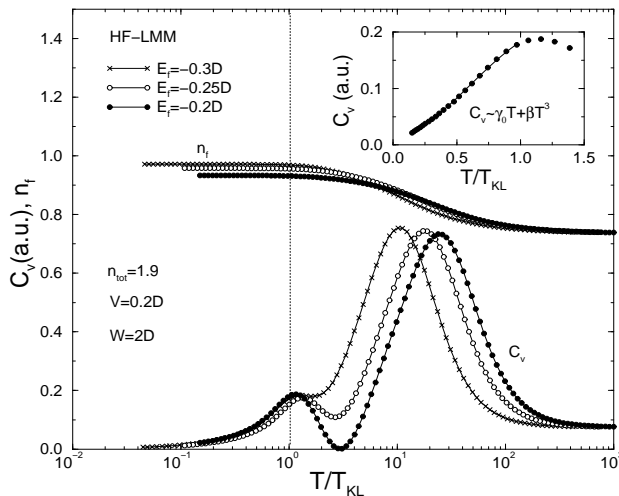


FIG. 11: Specific heat and occupation numbers of f electrons vs. T/T_{KL} in the HF-LMM regime. The inset presents the $T/T_{KL} < 1$ region, showing a cubic contribution $C_v \propto \gamma_0(T/T_{KL}) + \beta(T/T_{KL})^3$.

In Fig. 12 we show the coefficient $\gamma(T) = C_v/T$ vs. T for the HF-LMM regime, and in the inset we show $\gamma(T) = C_v(T)/T$ vs T/T_{KL} . The reduction of the effective masses $m^* \propto \gamma_0$ corresponds to the crossover from the HF-LMM regime to Steglich's stable moment regime (SMR) corresponding^{4,5} to $g \ll 1$. The reduction of the effective mass is again associated to the decrease of $\rho_{f,\sigma}(\mu)$ at very low temperatures ($T < T_{KL}$).

In Fig. 13 we present in a linear scale the same results of Fig. 12 at $T \sim T_{KL}$, but only for $E_f = -0.20D$. The inset shows the linear behavior of $(\gamma(T) - \gamma_0)$ vs. T^2 , corresponding

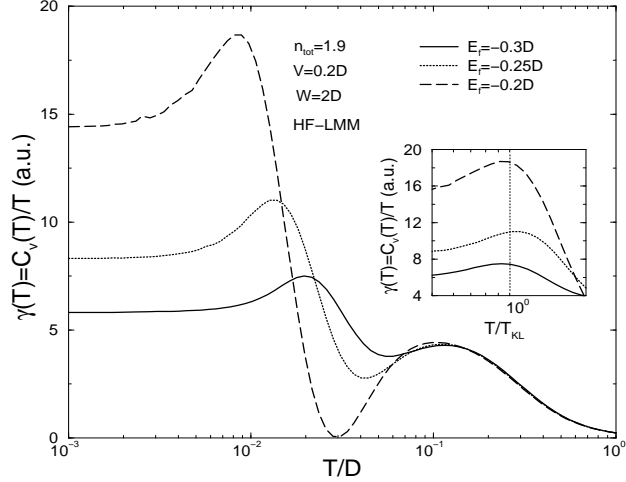


FIG. 12: Sommerfeld's coefficient $\gamma(T) = C_v(T)/T$ vs. T in the HF-LMM regime at very low temperatures. The coefficient $\gamma(T)|_{T=0.0} = \gamma_o \propto m^*$, where m^* is the reduced mass of the quasi-particles.

FIG. 13: Sommerfeld's coefficient $\gamma(T) = C_v(T)/T$ vs. T in the HF-LMM regime at very low temperatures. The inset shows the linear behavior of the $(\gamma(T) - \gamma_o)$ vs. T^2 associated with Sommerfeld's second term in the T expansion of C_V .

to the cubic dependence of C_V discussed above.

1. Discussion

It is clear that our method does not give the Kondo peak nor the quenching of the magnetic moment in the HF-LMM region. This is the region where the RKKY interactions

override the Kondo effect, and one is not quite clear of what should be the exact paramagnetic solution in that region. The Kondo resonance is observed in some theoretical calculations of the paramagnetic region with a moderately small value of Steglich's parameter $g^{4,5}$, like in Fig. 3f of reference 7, but we are not certain that these calculations correspond to the HF-LMM region. We must also consider that we have not included explicit magnetic interactions into the Hamiltonian, and also that there is no RKKY interaction because only second order cumulants are employed in the basic CHA expansion, as shown by the corresponding diagrams (see e.g. Fig. 1 or reference 16).

The absence of fourth and higher order cumulants in the CHA leads to a disturbing question: how do we obtain any Kondo resonance at all in the HF-K region, if apparently there are no spin flip processes in our calculation? To answer this question we notice that although the X-boson method starts from an expansion without spin flips, it is followed by a minimization of the free energy with respect to $R = \langle X_{00} \rangle$, with the completeness as a subsidiary condition (cf. Eq. (4) of reference 16). In this procedure the original solution is modified so that it gives the best possible physical solution (as regards to the free energy F) compatible with the general form of the CHA. The shifting of the localized energy E_f to the renormalized value $\widetilde{E}_f = E_f + \Lambda$ optimizes the free energy F giving at the same time a peak near the chemical potential μ , that takes the place of the Kondo resonance when parameters in the HF-K region are used. This result is not achieved in the HF-LMM region because the required shift E_f would not minimize F , and one is then left with an unquenched doublet without the corresponding spectral density increase around μ . A complementary explanation is that the constrained minimization would correspond to adding to the CHA expansion an extra number of undefined higher order diagrams, that would result in the formation of the Kondo resonance and of the quenching of the magnetic moment by the conduction electrons in the HF-K region.

We should point out that the same type of arguments presented here would also apply to the SBMFT, because after making the mean field approximation of the slave boson operator, one is left with two hybridized bands without any explicit correlation, and it is again the free energy restrained minimization that leads to the formation of a resonance that describes the Kondo peak.

IV. SUMMARY AND CONCLUSIONS

We employed the X-boson technique to calculate the specific heat of the PAM in two regimes (HF-K and HF-LMM), and we find agreement with recent theoretical work^{6,7,8,13,14,15} as well as qualitative agreement with measurements^{4,5} of Sommerfeld's coefficient $\gamma(T) = C_v(T)/T$. The low temperature entropy shows a crossover from a singlet ground state in the HF-K regime to a lattice of doublets in the HF-LMM region, and we discuss the origin of this behavior. We conclude that our method gives fairly good results in the Kondo region not very far from the intermediate valence region, as well as in this last region.

The specific heat in the HF-LMM region has a $C_v(T) \sim \beta T^3$ contribution, that can be attributed to Sommerfeld's second term in the temperature expansion of C_V . It would be interesting to calculate the electrical resistivity in the two regimes at low temperatures ($T < T_0$).

Acknowledgments

We would like to express our gratitude to Prof. Eduardo Miranda and to Prof. Ben Hur Bernhard for several helpful discussions. The financial support of the São Paulo State Research Foundation (FAPESP), the National Research Council (CNPq) and the Latin American Center of Physics (CLAF) is gratefully acknowledged.

APPENDIX A: THE ENTROPY OF THE PAM FOR VERY HIGH T

When $T \rightarrow \infty$ one is tempted to consider a uniform occupation of all the states, but we shall show that this is only true when the chemical potential is kept constant. This assumption is not generally true for a system with a fixed total number $n_{tot} = N_{tot}/N_S$ of electrons per site (N_S is the number of sites), and we shall calculate the entropy in this limit as a function of n_{tot} .

When $T \rightarrow \infty$ we can set (we take $k_B = 1$) $V/T = W/T = 0$, and we can write the thermodynamic potential per site

$$\begin{aligned} \frac{\Omega}{N_S} &= T \ln [(1 + 2 \exp[-(E_f - \mu)/T]) \\ &\times (1 + \exp[+\mu/T])^2], \end{aligned} \tag{A1}$$

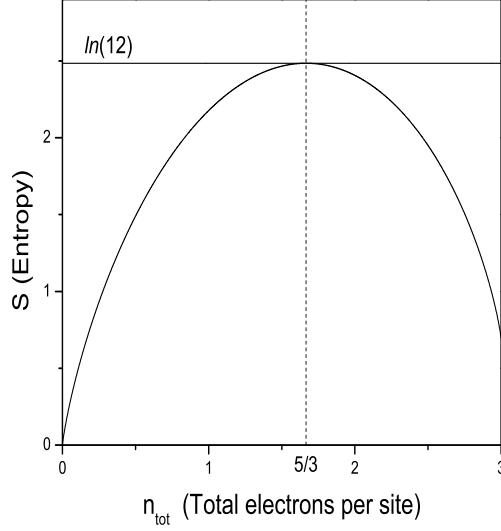


FIG. 14: Entropy per site of the PAM for $T \rightarrow \infty$ as a function of the total number of electrons per site $y = n_{tot}$. The horizontal line corresponds to $S_{T \rightarrow \infty}(5/3) = \ln(12)$.

and

$$n_{tot} = \frac{2 \exp[-(E_f - \mu)/T]}{1 + 2 \exp[-(E_f - \mu)/T]} + \frac{2 \exp[+\mu/T]}{1 + \exp[+\mu/T]}. \quad (\text{A2})$$

For convenience we write

$$\begin{aligned} x &= \exp[-\mu/T], \\ y &= n_{tot}, \\ e_f &= \exp[E_f/T] \end{aligned} \quad (\text{A3})$$

so that Eq. (A2) can be written as

$$y = \frac{2}{e_f x + 2} + \frac{2}{x + 1}. \quad (\text{A4})$$

As we are interested in the limit $T \rightarrow \infty$ we write here $e_f = 1$, and solve x as a function of y :

$$x = \frac{(4 - 3y + \sqrt{16 + y^2})}{2y}. \quad (\text{A5})$$

The solution with $-\sqrt{16 + y^2}$ gives negative values of x and we have to bound the total number of electrons $n_{tot} = y$ to the interval $[0, 3]$, i.e. only take

$$0 \leq y \leq 3. \quad (\text{A6})$$

It is clear that except for $x = 1$ (which corresponds to $n_{tot} = 5/3$) we have $\mu = \alpha T$, that goes to infinity together with T , and from Eq. (A4) or Eq. (A5) follows that the value of α has the sign of $(n_{tot} - 5/3)$.

The thermodynamic potential and the entropy can now be calculated for $T \rightarrow \infty$ as a function of $y = n_{tot}$. The expression for the entropy is

$$S_{T \rightarrow \infty}(y) = y \ln \left[\frac{4 - 3y + \sqrt{16 + y^2}}{2y} \right] + \ln \left[\frac{(4 - y + \sqrt{16 + y^2})^2 (4 + y + \sqrt{16 + y^2})}{(4 - 3y + \sqrt{16 + y^2})^3} \right] \quad (\text{A7})$$

and is plotted in figure 14.

The entropy for $n_{tot} = 1.6$ is $S_{T \rightarrow \infty}(1.6) = 0.998765 \ln(12)$ (see figure 3) while for $n_{tot} = 1.9$ is $S_{T \rightarrow \infty}(1.9) = 0.984597 \ln(12)$ (see figure 9). It follows from Eq. (A1) that for $T \rightarrow \infty$ it is

$$n_f = \frac{2}{2+x} \quad \text{and} \quad n_c = \frac{2}{1+x}, \quad (\text{A8})$$

where as before $x = \exp[-\mu/T]$.

* Electronic address: rfranco@if.uff.br

† Electronic address: figueira@if.uff.br

‡ Electronic address: foglio@ifi.unicamp.br

¹ J. Kondo, in *Solid State Physics* **23**, 183 (1969).

² C. Kittel, in *Quantum Theory of Solids*, Wiley, New York (1963).

³ M. A. Continentino, in *Quantum Scaling in Many Body Systems*, World Scientific, Singapore (2001).

⁴ N. Grewe and F. Steglich, in *Handbook on the Physics and Chemistry of Rare Earts*, Vol **14**, Edited by K. A. Gschneider Jr. and L. Eyring (Elsevier, Amsterdam) (1991).

⁵ F. Steglich, C. Geibel, K. Gloss, G. Olesch, C. Schank, C. Wassilew, A. Loidl, A. Krimmel and G. R. Stewart, *J. Low Temp. Phys.* **95**, 3 (1994).

⁶ B. H. Bernhard, C. Lacroix, J. R. Iglesias and B. Coqblin, *Physica B* **259-261**, 227 (1999) ; B. H. Bernhard, C. Lacroix, *Phys. Rev. B* **60**, 12149 (1999).

- ⁷ Luo H. G. and Wang S. J., Phys. Rev. B **62**, 1485 (2000).
- ⁸ Peres N. M. R., Sacramento P. D. and Araujo M. A. N., Phys. Rev. B. **64**, 113104 (2001).
- ⁹ Coleman P., Phys. Rev. B. **29**, 3035 (1984).
- ¹⁰ Coleman P., J. Magn. Magn. Mat. **47 & 48**, 323 (1985).
- ¹¹ D. M. Newns, N. Read, Advances in Physics, **36**, 799 (1987).
- ¹² A. Georges, G. Kotliar, W. Krauth and M. J. Rozenberg, Rev. Mod. Phys. **68**, 13 (1996).
- ¹³ Th. Pruschke, R. Bulla and M. Jarrell, Phys. Rev. B **61**, 12799 (2000).
- ¹⁴ T. A. Costi and N. Manini, J. Low. Temp. Phys, **126**,835 (2002).
- ¹⁵ S. Burdin, A. Georges and D Grepel, Phys. Rev. Lett. **85**, 1048 (2000).
- ¹⁶ R. Franco, M. S. Figueira and M. E. Foglio, Phys. Rev. B. **66**, 045112 (2002).
- ¹⁷ R. Franco, M. S. Figueira and M. E. Foglio, Physica A. **308**, 245 (2002).
- ¹⁸ R. Franco, M. S. Figueira and M. E. Foglio, J. Magn. Magn. Mat. **226 & 230**, 194 (2001).
- ¹⁹ P. Coleman, Phys. Rev. B **35**, 5072 (1987).
- ²⁰ Figueira M. S. , Foglio M. E. and Martinez G. G., Phys. Rev. B **50**, 17933 (1994).
- ²¹ M. E. Foglio and M. S. Figueira, J. Phys. A: Math. Gen. **30**, 7879 (1997).
- ²² M. E. Foglio and M. S. Figueira, International Journal of Modern Physics B **12**, 837 (1998).
- ²³ C. M. Varma, Comments on Condensed Matter Physics, **11**, 221 (1985).
- ²⁴ Schrieffer and Wolff, Phys. Rev. **149**, 491 (1966).
- ²⁵ As in our present derivation we can not determine g_c , the HF-K or HF-LMM character of the system can be only inferred from their calculated properties.
- ²⁶ T. A. Costi, Phys. Rev. Lett. **85**, 1504 (2000). In this reference, as well as in Appendix B of reference [14] it is shown how to obtain, for a Kondo lattice, the part of the f -spectrum lying close to the Fermi level and associated to the Kondo resonance.
- ²⁷ A. Amato, D. Jaccard, J. Fluoquet, F. Lapierre, J. L. Tholence, R. A. Fisher, S. E. Lacy, J. A. Olsen and N. E. Phyllips, J. Low. Temp. Phys, **68**,371 (1987).
- ²⁸ F. Steglich, U. Rauchschwalbe, U. Gottwick, H. M. Mayer, G. Sparn, N. Grewe, U. Poppe and J. J. M. Franse, J. Appl. Phys, **57**, 3054 (1985).
- ²⁹ A. Benoit, A. Berton, J. Chaussy, J. Flouquet, J. C. Lasjaunias, J. Odin, J. Palleu, J. Peyrard and M. Ribault, in *Valence Fluctuations in Solids*, Edited by L. M. Falicov, W. Hanke and M. B. Maple (Not Holland, Amsterdam), 283 (1981).
- ³⁰ Bredl C. D. , Horn S., Steglich F. , Luthi B. and Martin R. M, Phys. Rev. Lett. **52**, 1982

(1984).

- ³¹ L. Rebersky, K. Reilly, S. Horn, H. Borges, J. D. Thompson, J. O. Willis, R. Aikin, R. Caspary and C. D. Bredl, *J. Appl. Phys.*, **63**, 3405 (1988).
- ³² K. Andres, J. E. Graebner and H. R. Ott, *Phys. Rev. Lett.* **35**, 1779 (1975).
- ³³ Z. Tesanovic and O. Valls, *Phys. Rev. B* **34**, 1918 (1986).
- ³⁴ J. S. Kim and G. R. Stewart, *Phys. Rev. B* **49**, 327 (1994).

